PCT WORLD INTELLECTUAL PROPERTY ORGANIZATION
International Bureau

INTERNATIONAL APPLICATION PUBLISHED UNDER THE PATENT COOPERATION TREATY (PCT)

(51) International Patent Classification 6 :		(11) International Publication Number:
G06K 9/00, 9/46, 9/48, 9/52, 9/38	A1	WO 95/15536
		(43) International Publication Date: 8 June 1995 (08.06.95)

(21) International Application Number: PCT/US94/13294

(22) International Filing Date: 30 November 1994 (30.11.94)

(30) Priority Data:
159,133 30 November 1993 (30.11.93) US

(71) Applicant: ARCH DEVELOPMENT CORPORATION [US/US]; The University of Chicago, 1101 East 58th Street, W213, Chicago, IL 60637 (US).

(72) Inventors: GIGER, Maryellen, L.; 658 Hillcrest, Elmhurst, IL 60126 (US). ARMATO, Samuel; 1005 E. 60th Street, Chicago, IL 60637 (US). MACMAHON, Heber; 1846 Sedgisick Street, Chicago, IL 60614 (US).

(74) Agents: KUESTERS, Eckhard, H. et al.; Oblon, Spivak, McClelland, Maier & Neustadt, P.C., 4th floor, 1755 Jefferson Davis Highway, Arlington, VA 22202 (US).

(81) Designated States: AM, AT, AU, BB, BG, BR, BY, CA, CH, CN, CZ, DE, DK, EE, ES, FI, GB, GE, HU, JP, KE, KG, KP, KR, KZ, LK, LR, LT, LU, LV, MD, MG, MN, MW, NL, NO, NZ, PL, PT, RO, RU, SD, SE, SI, SK, TJ, TT, UA, UZ, VN, European patent (AT, BE, CH, DE, DK, ES, FR, GB, GR, IE, IT, LU, MC, NL, PT, SE), OAPI patent (BF, BJ, CF, CG, CI, CM, GA, GN, ML, MR, NE, SN, TD, TG), ARIPO patent (KE, MW, SD, SZ).

Published
With international search report.
Before the expiration of the time limit for amending the claims and to be republished in the event of the receipt of amendments.

(54) Title: AUTOMATED METHOD AND SYSTEM FOR THE DETECTION OF GROSS ABNORMALITIES AND ASYMMETRIES IN CHEST IMAGES

(57) Abstract

A method for the automated detection of gross abnormalities and asymmetries in chest images (10), including generating image data from radiographic images of the thorax. The image data are then analyzed in order to produce the boundaries of the aerated lung regions in the thorax. This analysis comprises location of the mediastinum and lung apices, iterative global thresholding (11) with centroid testing of contours, local thresholding (12) on regions along initial contours of the aerated lung, correction (13) for regions near the costo and cardiophrenic angles in the chest, analysis (15) of the areas and density distribution within the aerated lung regions in the chest and determination (16) of the likelihood of the presence of a gross abnormality or asymmetry. Finat ouptut could be the computer determined contours of the lungs or the likelihood for abnormality.

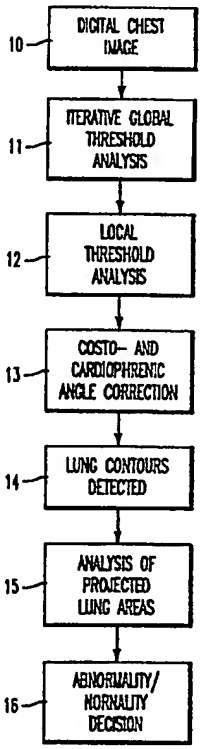

BEST AVAILABLE COPY

FOR THE PURPOSES OF INFORMATION ONLY

Codes used to identify States party to the PCT on the front pages of pamphlets publishing international applications under the PCT.

AT	Austria	**GB**	United Kingdom	**MR**	Mauritania
AU	Australia	**GE**	Georgia	**MW**	Malawi
BB	Barbados	**GN**	Guinea	**NE**	Niger
BE	Belgium	**GR**	Greece	**NL**	Netherlands
BF	Burkina Faso	**HU**	Hungary	**NO**	Norway
BG	Bulgaria	**IE**	Ireland	**NZ**	New Zealand
BJ	Benin	**IT**	Italy	**PL**	Poland
BR	Brazil	**JP**	Japan	**PT**	Portugal
BY	Belarus	**KE**	Kenya	**RO**	Romania
CA	Canada	**KG**	Kyrgystan	**RU**	Russian Federation
CF	Central African Republic	**KP**	Democratic People's Republic of Korea	**SD**	Sudan
CG	Congo			**SE**	Sweden
CH	Switzerland	**KR**	Republic of Korea	**SI**	Slovenia
CI	Côte d'Ivoire	**KZ**	Kazakhstan	**SK**	Slovakia
CM	Cameroon	**LI**	Liechtenstein	**SN**	Senegal
CN	China	**LK**	Sri Lanka	**TD**	Chad
CS	Czechoslovakia	**LU**	Luxembourg	**TG**	Togo
CZ	Czech Republic	**LV**	Latvia	**TJ**	Tajikistan
DE	Germany	**MC**	Monaco	**TT**	Trinidad and Tobago
DK	Denmark	**MD**	Republic of Moldova	**UA**	Ukraine
ES	Spain	**MG**	Madagascar	**US**	United States of America
FI	Finland	**ML**	Mali	**UZ**	Uzbekistan
FR	France	**MN**	Mongolia	**VN**	Viet Nam
GA	Gabon				

Description

Automated Method and System for The Detection of Gross Abnormalities and Asymmetries in Chest Images

The present invention was made in part with U.S. Government support under NIH grants/contracts CA48985 and CA09649; Army grant/contract DAMD 17-93-J-3021; and American Cancer Society grant/contract FRA-390. The U.S. Government has certain rights in the invention.

Technical Field

The invention relates to a method and system for the computerized automatic detection of gross abnormalities and asymmetries in chest images, and more specifically to a method and system for detection in digital chest radiographs. Asymmetries are detected by multiple stages of global and local gray-level thresholding along with contour detection. Abnormalities are detected based on deviation from expected symmetries between the left and right lungs, using such features as size and density of the aerated lung regions.

Background Art

Computer-aided diagnosis (CAD) has potential to become a valuable tool for detecting subtle abnormalities in chest radiographs. It would be useful for a CAD scheme to detect more large-scale abnormalities, which commonly cause abnormal asymmetry on the radiograph. In general, asymmetric abnormalities appear as a substantial decrease in the area of aerated lung in one hemithorax. This would include interstitial infiltrates, dense air space infiltrates, pleural effusions, large masses, or unilateral emphysema.

Most CAD schemes currently employed in digital chest radiography are specific to one particular and often localized

pathology, for example lung nodule, interstitial infiltrate, pneumothorax or cardiomegaly. These schemes often utilize *a priori* information regarding the "normal" appearance of the ribcage, diaphragm and mediastinum in a digital chest radiograph. A potential problem arises when the nature of the thoracic abnormality is such that it substantially affects the volume of the lungs. An abnormality of this type will usually cause a decrease in the aerated lung region (i.e. the high optical density associated with the normally low attenuation of the lungs) as projected onto the radiograph. This can substantially alter the overall morphology of the chest, resulting in potential failure of such CAD schemes. Detection of these abnormalities may also prove useful in prioritizing abnormal cases in a picture archiving and communication system (PACS).

The present application discloses a technique for the automated detection of abnormal asymmetry in digital chest radiographs. The method consists of an iterative global thresholding technique in conjunction with a contour detection algorithm to construct an initial set of contours around the two projected aerated lung regions in a chest image. In order to identify the lungs more accurately, a local thresholding technique is then applied within regions of interest (ROIs) centered along the contours that result from the global thresholding. The areas and densities of the two lung regions identified in this manner can be compared in order to determine whether an asymmetric abnormality is present.

Disclosure of the Invention

Accordingly, an object of this invention is to provide an automated method and system for detecting and displaying gross abnormalities and asymmetries in medical images of the chest.

Another object of this invention is to provide an automated method and system for the iterative gray-level thresholding of lung regions in a chest image.

Another object of this invention is to provide an automated method and system for the local thresholding of lung regions in a chest image.

Another object of this invention is to provide an automated method and system for defining the edge of the aerated lung regions by using features based on the anatomic structure of the lung and its surround.

Another object of this invention is to provide an automated method and system for the detection of lung boundaries within a radiographic image of the thorax.

Another object of this invention is to provide an automated method and system for the extraction of objects (features) within the lung regions in chest images of the thorax by using size and shape of the aerated lung regions..

Another object of this invention is to provide an automated method and system for distinguishing abnormal regions from normal anatomy based on asymmetries between the left and right lung regions.

These and other objects are achieved according to the invention by providing a new and improved automated method and system in which an iterative, multi-level gray level thresholding is performed, followed by a local thresholding and an examination of regions based on anatomically-based features, and then followed by an analysis of the possible asymmetries. For example, asymmetric abnormalities may present on the chest radiograph as a decrease in the area of aerated lung in one hemithorax and in different degrees of subtlety due to size and composition. In order to allow the various abnormalities to be detected, the aerated areas are analyzed and compared with the opposing hemithorax.

Brief Description of the Drawings

A more complete appreciation of the invention and many of the attendant advantages thereof will be readily obtained as the same becomes better understood by reference to the following detailed description when considered in connection with the accompanying drawings, wherein:

FIG. 1 is a schematic diagram illustrating the automated method for detection of asymmetric abnormalities according to the invention;

FIG. 2 is a schematic diagram illustrating the automated method for the iterative, global thresholding for the detection of the boundary of the thorax according to the invention;

FIG. 3 is a graph illustrating the gray-level histogram of a chest image indicating the computer-determined location of the lung peak and the minimum between the lung and mediastinum peaks; This represents the range of gray values used in the iterative thresholding technique.

FIGS. 4A-4E shows binary images created by thresholding a chest image at different gray values;

FIG. 5 is a graph showing the empirically-determined centroid limits plotted on image-based coordinates, where contours with centroids outside this limit are eliminated from the image;

FIG. 6 is a schematic diagram illustrating the automated method for the local thresholding for the detection of the boundary of the thorax according to the invention;

FIG. 7 is a schematic diagram showing the placement of ROIs for local threshold analysis along the initial contours that result from the iterative global threshold process;

FIGS. 8A and 8B are diagrams illustrating local threshold analysis;

FIGS. 9A and 9B are schematics illustrating the features (area and density, respectively) extracted for use in the comparison of the left and right aerated lung regions;

FIG. 10 is a schematic diagram illustrating the automated method for comparison of left and right lung regions and the determination of the presence of an abnormality;

FIG. 11 is a graph of the left lung area plotted as a function of right lung area for 70 cases. The regression line shown is based on true normal cases only;

FIG. 12 is a graph illustrating the ROC curve showing the performance of the method in detecting gross abnormalities and asymmetries; and

FIG. 13 is a schematic block diagram illustrating a system for implementing the automated method for the detection of gross abnormalities and asymmetries in chest images.

Best Mode for Carrying Out the Invention

Referring now to the drawings, and more particularly to FIG. 1 thereof, a schematic diagram of the automated method for the detection of gross abnormalities and asymmetries in chest images is shown. The overall scheme includes an initial acquisition of a radiograph of the thorax and digitization to produce a digital chest image (step 10). Detection of aerated lung boundaries is performed initially using an iterative, global thresholding technique (step 11) which includes a centroid test. After which, the initial contours are used for positioning of the ROIs for a local thresholding technique (step 12). After the local thresholding procedure, there is a correction for the costo- and cardiophrenic angle (step 13). The lung contours are then determined (step 14). By analyzing the resulting contours and the projected lung areas (step 16), the chest image is assigned a likelihood of having a gross abnormality or asymmetry (step 16).

Figure 2 shows a schematic diagram illustrating the automated method for the iterative global thresholding for the detection of the boundary of the thorax. Initially, horizontal gray-level profiles in the image are calculated (step 20) and used to determine the location of the mediastinum and the lung apices. This information is used throughout the scheme in order to differentiate the right hemithorax from the left and to identify an upper bound in the image that prevents the contours from growing along the neck. This information is required for each image to compensate for differences in patient positioning.

A global gray-level histogram is used to initially segment the lungs in the chest image (step 21). In an effort to obtain more uniform histograms, the calculation of the histogram is effectively centered over the thorax. In this example, a 181x141 pixel region centered 70 pixels from the top of the image, i.e. over the thorax, was chosen. Step 22 of the method shown in FIG. 2 where the lung and mediastinum peaks are located will now be described. The typical histogram (FIG. 3) resulting from such a region exhibits two peaks 30 and 31: one centered over lower gray values that corresponds to pixels predominantly within the lungs, and another centered over higher gray values that corresponds to pixels predominantly in the mediastinum, in the ribcage edge, and, presumably, in any asymmetric abnormality that may be present, respectively.

The goal with regard to performing global threshold analysis, therefore, is to use the histogram in order to determine an appropriate gray value that separates the gray values belonging to pixels within the aerated lung region from those that are located outside the lungs. The task of determining an appropriate threshold proved to be impossible based on the selection of a single gray value. Values were either too low and the resulting binary image insufficiently captured the lung regions, or the values were too high and the

lung regions merged with regions outside the lungs; in most cases, a certain threshold value resulted in the former condition in one area of the lung region and in the latter condition in another area.

This problem is overcome by introducing an iterative global threshold scheme. Instead of choosing one gray-level threshold value, a range of values is used in succession. The running slope (first derivative) of the global gray-level histogram is used in order to identify the gray value at which the peak (30 in FIG. 3) corresponding to the lung regions occurs and the gray value at which the minimum between the lung and mediastinum peaks occurs (32 in FIG. 3). A number of equally-spaced gray values between this peak and minimum are then each used in a threshold iteration. In this example 7 gray values were detected. A typical histogram along with the range of gray-level thresholds used during the iterative global gray-level thresholding is shown in Figure 3.

The iterations are used to create a binary image (step 23). The first iteration creates a binary image by using the smallest of the seven gray values (i.e. the highest optical density of the range) as the threshold limit. Pixels are turned "on" in the binary image if the corresponding pixel in the image has a gray value greater than a certain level above the background level, such as 10, but less than this threshold limit. FIGS. 4A-4E illustrates, schematically, the binary images that result from applying four different gray-level thresholds to a chest image.

In FIG. 4A, the result of thresholding at a smaller threshold is shown. The actual lung boundary 40 is shown for reference only. The thresholding produces a number of regions 41 within the lung boundary 40 and a region 42 outside of the boundary 40. The region 42 is eliminated by a centroid check described below.

The resulting binary image is sent to the contour detection routine, which utilizes a connectivity scheme (such

as 8-point) to identify contours representing the boundaries of groups of contiguous "on" pixels (step 24). Connectivity schemes are described, for example, in "Automatic segmentation of liver structure in CT images," by K. Bae, M. L. Giger, C. T. Chen, and C. Kahn, (Medical Physics 20, 71-78 (1993)). The routine also calculates important geometrical properties of these contours, such as the centroid of the contour, contour compactness, contour length (in terms of pixels), and the area enclosed within the contour (in terms of pixels).

The centroid of a contour is used to determine whether the pixels within that contour are within a region that is likely to contain lung (step 25). A "centroid limit" can be empirically constructed by analyzing the centroids of all contours resulting during all of the threshold iterations. The limit, shown in FIG. 5, is based on the spatial distribution in the image plane of the centroids of contours falling within the lung regions and the centroids of contours external to the lungs for 28 chest images. If the centroid of a contour falls outside this limit, the pixels enclosed by this contour are turned "off" (such as region 42 in FIG. 4A). These external regions are thus prevented from merging with regions within the lungs at later iterations where the threshold gray value is greater and the likelihood of such a merge is increased. This allows for the most complete identification of the lungs without also incorporating extraneous area.

This process of thresholding to create a binary image, identifying contours, and turning pixels "off" based on a centroid check is repeated for each of the iterations, with the threshold gray value used to produce the binary image increasing at each iteration. FIGS. 4B-4D show the results of subsequent iterations. In FIG. 4B, larger regions 43 are determined within the lung boundary 40 along with a region 44 which is also eliminated by the centroid check. Larger regions 45 are determined within the lung boundary 40 shown in

FIG. 4C. Also shown in FIG. 4C is a region 46 which contains pixels outside of the lung boundary 40, but is not eliminated by the centroid check as it has a centroid within the limit 51 as shown in FIG. 5. FIG. 4D shows an iteration at a higher pixel value where the regions 47 and 48 are now closely approximating the lung boundary 40. The iterative thresholding technique can be thought of as finding the perimeter of a mountain range at various heights, with lower threshold values being closer to the top of the mountain range.

It should be pointed out that a more strict centroid limit could be employed during the later iterations, since the spatial distribution of lung contours typically becomes more confined as the threshold level is increased. The stricter centroid limit shown as 51 in Figure 5 could eliminate regions such as region 46.

A morphological open operation with a 3x3 kernel is also applied during each of the final two iterations (step 26). The morphological open operation is described in, for example, *Image Analysis and Mathematical Morphology* by J. Serra (Academic, New York, 1982). This combination of an erosion filter followed by a dilation filter eliminates many of the slender artifacts that remain "on" in the binary image as a result of the process that turns "off" regions of the image based on the centroid check. Thus as shown in FIG. 4E, the morphological open operation can eliminate the slender portion 49 of region 48 to give contours 50. The final result of the global threshold iterations is an initial set of contours representing the aerated lung regions in the image (step 27).

It was found that these initial contours tended to under-represent the actual lung regions. Since increasing the largest threshold gray value produced more artifacts in the resulting contours, a local thresholding scheme is applied to the output of the global thresholding scheme. Figure 6 illustrates schematically the method for the local

thresholding. Overlapping ROIs pixels are centered along the initial contours (step 60). In this example ROIs of dimension 31x31 were centered at every thirtieth point. Other sizes and spacing are possible. FIG. 7 schematically shows the placement of ROIs 70 along the lung contours 71. The pixels within each ROI are then turned "on" or "off" to form a binary image based on a threshold gray value determined individually for each ROI.

As shown in FIG. 6, it is determined in step 61 whether the ROIs are located on a lateral aspect of the lung. For ROIs along the medial and diaphragmatic aspects of each lung region, the mean pixel value within the ROI is selected as the threshold (step 62). For ROIs along the lateral aspect, a gray level histogram is constructed (step 63), and the initial choice of threshold is set equal to the gray value at which the histogram minimum with the largest gray value occurs. The threshold value actually used for the lateral ROIs is then an average of the initial threshold values of the ROI and its two neighboring ROIs. Thus the threshold values for each of the ROIs is determined by repeating the operation for all ROIs (step 64).

The local thresholding is described in more detail in FIG. 8A and 8B. FIG. 8A shows a histogram of a ROI such as 70 (see FIG. 7), while FIG. 8B shows a histogram of a ROI such as 74. The bimodal distribution results from the overlap of the contour, which produces valleys 80 and 81. In the local thresholding, the gray value p_i of the center pixel of the ROI is replaced with one of two selected gray values depending on whether $p_i < p_{valley}$ or $p_i \geq p_{valley}$. Or,

$$p(x,y) = \begin{cases} 1 & \text{if } p(x,y) \geq \text{threshold cutoff of ROI centered at } p(x,y) \\ 0 & \text{if } p(x,y) < \text{threshold cutoff of ROI centered at } p(x,y) \end{cases}$$

Instead of 1, p(x,y) could be left unchanged. This local thresholding thus provides a binary image.

The method, however, may under-represent the costophrenic angle and over-represent the cardiophrenic angle. To accommodate these important anatomical landmarks, two additional ROIs (72 and 73 in FIG. 7) are added to better capture the costophrenic angle, while the criterion for setting the threshold within the ROI overlaying the cardiophrenic angle was altered to yield a lower threshold value when necessary (step 65).

The binary image constructed by thresholding individual ROIs in this manner is sent to the contour detection routine, the morphological open operation is again applied, and the resulting final contours (step 66) are superimposed on the original image (step 67).

The analysis of the projected lung areas (step 15 in FIG. 1) will now be described. The calculated areas and densities of the final contours, corresponding to the projected areas of the aerated lung regions, can then used to make a decision regarding the presence of an asymmetric abnormality (step 16 in FIG. 1). These features are schematically described in FIGS. 9A and 9B. In FIG. 9A, the determined contours 90 are shown along with the actual lung boundaries 40. The area of contours to the left and the right of the mediastinum (steps 100 and 101) (the area within each of the left and right lung contours) is calculated (i.e. the pixels are counted). The decision criterion is based on a comparison of the right lung area and left lung area (step 102), which are defined as the sum of the areas of all contours to the right and left of the mediastinum, respectively. Figure 10 shows schematically the method for the comparison of the left and right aerated lung regions. Presumably, all contours outside the lung region are suppressed, and large abnormalities may result in the aerated portion of the lung being divided into two or more regions.

The scheme was applied to a database of 35 normal cases, and an average right lung area to left lung area ratio (referred to as the area ratio measure) was calculated along

with the standard deviation of the ratio. In addition, a regression line was constructed based on the relationship between the left lung area and the right lung area for these normal cases (step 93), as shown in Figure 11. The average perpendicular distance from the regression line of each point corresponding to a normal case in this plot was calculated along with the standard deviation of that distance. A distance threshold from the regression line is used to determine the finding of abnormality. Figure 12 shows the performance of the method with a ROC curve.

Also shown in FIG. 10 is the area analysis. The average pixel density is calculated for a number of regions in each lung contour (steps 104 and 105). The number and actual locations of the division of the areas can be empirically derived. The lung contours 90 of FIG. 9A have be divided to obtain lung contours 91 in FIG. 9B. In this example the number of regions was selected as three, and the location of the divisions are as shown. A density ratio is determined and compared to the density of normal cases (step 106). A regression line analysis similar to that described with respect to the area analysis is performed (step 107). The abnormality decision is based on a finding of abnormality in either of the area or density analysis (step 108).

Figure 13 is a more detailed schematic block diagram illustrating a system for implementing the method of the invention. Referring to Figure 13, radiographic images of an object are obtained from an image acquisition device 130, such as an x-ray device and laser digitizer, and input to the system. Each chest image is digitized by device 130 and put into memory 131. The image data is first passed through the iterative global thresholding circuit 132, which utilizes temporary image memory 133 during the iterations, and then the image data undergoes centroid checking centroid analysis circuit 134 in order to determine the initial boundary of the aerated lung regions. The data is passed to the local

thresholding circuit 135, which uses temporary memory 136 during the thresholding, and the correction circuit for the costo- and cardiophrenic angle 137 in order to determine the final boundary of each lung region. Image data within each lung region is passed to the sizing circuit 138 and the density-analysis circuit 139 in order to determine the area and density features for input to the comparison circuit 140. During the comparison of the aerated lung regions, the data is retained in image memory 141. In the superimposing circuit 142 the results are either superimposed onto chest images or given in text format. The results are then displayed on the display system 144 after passing through a digital-to-analog converter 143. The system according to the method can be implemented in both software and hardware, such as a programmed microprocessor or computer.

Obviously, numerous modifications and variations of the present invention are possible in light of the above technique. It is therefore to be understood that within the scope of the appended claims, the invention may be practiced otherwise than as specifically described herein. Although the current application is focused on gross abnormalities and asymmetries in chest, the concept can be expanded to the detection of abnormalities in other organs in the human body.

Claims

1. A method for detecting an abnormality in a radiographic image, comprising:

obtaining a radiographic image of a subject;

detecting a boundary of a feature in said radiographic image;

determining geometric descriptors of said feature; and

determining whether an abnormality exists in said feature using said geometric descriptors.

2. A method as recited in Claim 1, wherein said step of detecting said boundary of said feature comprises performing global gray-level thresholding on said radiographic image.

3. A method as recited in Claim 2, wherein said step of performing global gray-level thresholding comprises:

determining horizontal gray-level profiles in said radiographic image; and

constructing a global gray-level histogram using said gray-level profiles.

4. A method as recited in Claim 1, wherein said step of detecting said boundary of said feature comprises:

performing iterative global gray-level thresholding on said radiographic image.

5. A method as recited in Claim 1, wherein said step of performing iterative global gray-level thresholding comprises:

constructing a gray-level histogram of said radiographic image;

performing a running slope of said gray-level histogram to obtain a smoothed gray-level histogram; and

determining a number of first gray-level threshold values at selected locations in said smoothed gray-level histogram.

6. A method as recited in Claim 5, further comprising:

creating respective binary images based on each of said number of first gray-level threshold values; and

detecting a region corresponding to said feature using said binary images.

7. A method as recited in Claim 6, wherein creating said respective binary images comprises turning off pixels in said image having a gray level less greater a respective one of said first gray-level threshold values.

8. A method as recited in Claim 6, further comprising:

defining a centroid limit in said radiographic image; and

eliminating said region if it has a centroid outside of said centroid limit.

9. A method as recited in Claim 6, comprising:

performing a morphological open operation on selected ones of said binary images.

10. A method as recited in Claim 6, comprising:

using said binary images to create an initial boundary of said feature; and

performing local gray-level thresholding using said initial boundary of said feature.

11. A method as recited in 10, wherein performing local gray-level thresholding comprises:

placing regions-of-interest having a plurality of pixels along said initial boundary;

determining a second gray-level threshold value for each said region-of-interest;

selecting pixels in said regions-of-interest based upon respective ones of said second gray-level threshold values to obtain selected pixels; and

forming a second binary image based upon said selected pixels.

12. A method as recited in Claim 11, comprising:

determining whether a first region-of-interest among said region-of-interests is located on a first predetermined portion of said initial boundary;

constructing a second gray-level histogram for pixels located within said first region-of-interest determined to be located on said predetermined portion of said initial boundary;

determining said second gray-level threshold value for said first region-of-interest using said second gray-level histogram;

determining whether a second region-of-interest among said region-of-interests is located on a second predetermined portion of said initial boundary; and

determining said second gray-level threshold value for said second region-of interest determined to be located on said second predetermined portion of said initial boundary based upon gray-level values of pixels located within said second region-of interest.

13. A method as recited in Claim 12, wherein determining said second gray-level threshold value for said first region-of-interest comprises:

locating a minimum in said second gray-level histogram; and

selecting said second gray-level threshold value for said first region-of-interest as a gray-value corresponding to said minimum.

14. A method as recited in Claim 13, comprising:

selecting said second gray-level threshold value for said first region-of-interest as a gray-level value corresponding

to a minimum in said second gray-level histogram having a greatest gray-level value.

15. A method as recited in Claim 14, comprising:

selecting a third gray-level threshold value for said first region-of-interest as an average of said second gray-level threshold value for said first region-of-interest and second gray-level values for two regions-of-interest neighboring said first region-of-interest.

16. A method as recited in Claim 11, comprising:

detecting a boundary of said second binary image;

performing a morphological open operation on said boundary; and

superposing said boundary on said radiographic image.

17. A method as recited in Claim 11, comprising:

detecting a boundary of said second binary image;

determining said geometric descriptors using said boundary of said second binary image;

detecting whether said abnormality exists using said geometric descriptors calculated using said boundary of said second binary image.

18. A method as recited in Claim 1, wherein determining said geometric descriptors comprises:

determining an area of said boundary of said feature; and

determining an average density of selected portions of said feature; and

wherein determining whether said abnormality exists comprises:

comparing said area of said boundary of said feature to an area determined for a normal feature; and

comparing said average density for each of said portions of said feature to corresponding portions of a normal feature.

19. A method as recited in Claim 18, wherein comparing said area and comparing said average density each comprises performing a regression line analysis.

20. A method for detecting an abnormality in a radiographic chest image, comprising:

obtaining a radiographic chest image of a subject;

detecting a boundary of lungs in said radiographic image;

determining geometric descriptors of said lungs; and

determining whether an abnormality exists in said lungs using said geometric descriptors.

21. A method as recited in Claim 20, comprising:

obtaining a radiographic chest image having a plurality of pixels;

determining horizontal gray-level profiles in said radiographic image; and

determining lung apices and mediastinum locations using said horizontal gray-level profiles.

22. A method as recited in Claim 20, comprising:

selectively positioning a first region-of-interest over the thorax in said radiographic chest image;

constructing a gray-level histogram using pixels in said first region-of-interest;

performing a running slope of said gray-level histogram to construct a smoothed gray-level histogram; and

determining a number of first gray-level threshold values at selected locations in said smoothed gray-level histogram.

23. A method as recited in Claim 22, further comprising:

creating respective binary images at each of said number of first gray-level threshold values; and

detecting a region corresponding to said lungs using said binary images.

24. A method as recited in Claim 23, comprising:

using said binary images to create an initial boundary of said lungs; and

performing local gray-level thresholding using said initial boundary of said lungs.

25. A method as recited in 24, wherein performing local gray-level thresholding comprises:

placing regions-of-interest having a plurality of pixels along said initial boundary;

determining a second gray-level threshold value for each said region-of-interest;

selecting pixels in said regions-of-interest based upon respective ones of said second gray-level threshold values to obtain selected pixels; and

forming a second binary image based upon said selected pixels.

26. A method as recited in Claim 25, comprising:

placing a region-of-interest over a costophrenic angle of said lungs; and

placing a region-of-interest over the cardiophrenic angle of said lungs.

27. A method as recited in Claim 25, comprising:

determining whether a first region-of-interest among said region-of-interests is located on a lateral aspect of said lung;

constructing a second gray-level histogram for pixels located within said first region-of-interest determined to be located on said lateral aspect of said lung;

determining said second gray-level threshold value for said first region-of-interest using said second gray-level histogram;

determining whether a second region-of-interest among said region-of-interests is located on at least one of a medial and diaphragmatic aspects of said lungs; and

determining said second gray-level threshold value for said second region-of-interest determined to be located on said second predetermined portion of said initial boundary based upon gray-level values of pixels located within said second region-of-interest.

28. A method as recited in Claim 27, wherein determining said second gray-level threshold value for said first region-of-interest comprises:

locating a minimum in said second gray-level histogram; and

selecting said second gray-level threshold value for said first region-of-interest as a gray-value corresponding to said minimum.

29. A method as recited in Claim 28, comprising:

selecting said second gray-level threshold value for said first region-of-interest as a gray-level value corresponding to a minimum in said second gray-level histogram having a greatest gray-level value.

30. A method as recited in Claim 25, comprising:

detecting a boundary of said second binary image;

determining said geometric descriptors using said boundary of said second binary image;

detecting whether said abnormality exists using said geometric descriptors calculated using said boundary of said second binary image.

31. A method as recited in Claim 30, wherein determining said geometric descriptors comprises:

detecting right and left lung boundaries;

determining an area of said right lung boundary and an area of said left lung boundary;

dividing said each of said right and left lung boundaries into a selected number of portions; and

determining an average density of pixels in each of said portions of said right and left lung boundaries;

and wherein determining whether said abnormality exists comprises:

determining a ratio of said area of said right lung boundary to said area of said left lung boundary;

comparing said ratio to a corresponding ratio determined for normal lungs; and

comparing said average density for each of said portions of said right and left lung boundaries to a corresponding average densities of normal lungs.

32. A method as recited in Claim 31, wherein comparing said ratio and comparing said average density each comprises performing a regression line analysis.

33. A method as recited in Claim 32, comprising:

determining a regression line based upon said areas of said left and right lung boundaries and upon areas for normal left and right lungs;

determining a threshold of a distance for a point from said regression line using said areas for normal left and right lungs; and

determining whether said abnormality exists based upon said threshold.

34. A method as recited in Claim 32, comprising:

determining a regression line based upon said densities of said portions of said left and right lung boundaries and upon said corresponding densities of said normal lungs; and

determining a threshold of a distance for a point from said regression line using said corresponding densities of said normal lungs; and

determining whether said abnormality exists based upon said threshold.

35. A method as recited in Claim 32, comprising:

determining a first regression line based upon said areas of said left and right lung boundaries and upon areas for normal left and right lungs;

determining a first threshold of a distance for a point from said regression line using said areas for normal left and right lungs;

determining a second regression line based upon said densities of said portions of said left and right lung boundaries and upon said corresponding densities of said normal lungs; and

determining a second threshold of a distance for a point from said regression line using said corresponding densities of said normal lungs; and

determining whether said abnormality exists based upon at least one of said first and second thresholds.

36. A system for detecting an abnormality in a radiographic image, comprising:

an image acquisition device;

an image memory connected to said image acquisition device;

an iterative global thresholding circuit connected to said image memory;

a local thresholding circuit connected to said iterative global thresholding circuit;

a sizing circuit connected to said local thresholding circuit;

a density circuit connected to said local thresholding circuit;

a comparison circuit connected to said sizing and density circuits; and

a display.

37. A system as recited in Claim 36, further comprising:

a centroid circuit connected between said iterative global thresholding circuit and said local thresholding circuit; and

a correction circuit connected between said local thresholding circuit and said sizing and density circuits.

38. A system as recited in Claim 36, wherein said iterative global thresholding circuit comprises:

means for constructing a gray-level histogram of said radiographic image;

means for performing a running slope of said gray-level histogram to obtain a smoothed gray-level histogram; and

means for determining a number of first gray-level threshold values at selected locations in said smoothed gray-level histogram.

39. A system as recited in Claim 36, wherein said iterative global thresholding circuit further comprises:

means for creating respective binary images at each of said number of first gray-level threshold values;

means for detecting a region corresponding to a feature in said radiographic image using said binary images; and

means for using said binary images to create an initial boundary of said feature.

40. A system as recited in Claim 39, wherein said local thresholding circuit comprises:

means for placing regions-of interest having a plurality of pixels along said initial boundary;

means for determining a second gray-level threshold value for each said region-of-interest;

means for selecting pixels in said regions-of-interest based upon respective ones of said second gray-level threshold values to obtain selected pixels; and

means for forming a second binary image based upon said selected pixels.

41. A system as recited in Claim 40, wherein said local thresholding circuit further comprises:

means for determining whether a first region-of-interest among said regions-of-interest is located on a first predetermined portion of said initial boundary;

means for constructing a second gray-level histogram for pixels located within said first region-of-interest determined to be located on said predetermined portion of said initial boundary;

means for determining said second gray-level threshold value for said first region-of-interest using said second gray-level histogram;

means for determining whether a second region-of-interest among said regions-of-interest is located on a second predetermined portion of said initial boundary; and

means for determining said second gray-level threshold value for said second region-of-interest determined to be located on said second predetermined portion of said initial boundary based upon gray-level values of pixels located within said second region-of-interest.

42. A system as recited in Claim 36, wherein:

said sizing circuit comprises means for determining an area of a boundary of said feature;

said density circuit comprises means for determining an average density of selected portions of said feature; and

said comparison circuit comprises:

means for comparing said area of said boundary of said feature to an area determined for a normal feature; and

means for comparing said average density for each of said portions of said feature to corresponding portions of a normal feature.

43. A system as recited in Claim 42, wherein comparison circuit further comprises means for performing a regression line analysis.

FIG. 1

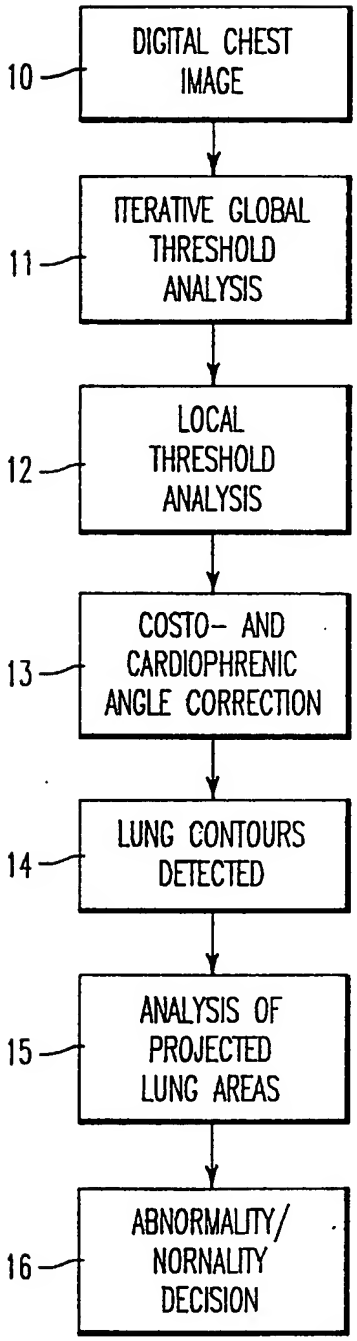
10
DIGITAL CHEST IMAGE
11
ITERATIVE GLOBAL THRESHOLD ANALYSIS
12
LOCAL THRESHOLD ANALYSIS
13
COSTO- AND CARDIOPHRENIC ANGLE CORRECTION
14
LUNG CONTOURS DETECTED
15
ANALYSIS OF PROJECTED LUNG AREAS
16
ABNORMALITY/ NORNALITY DECISION

FIG. 2

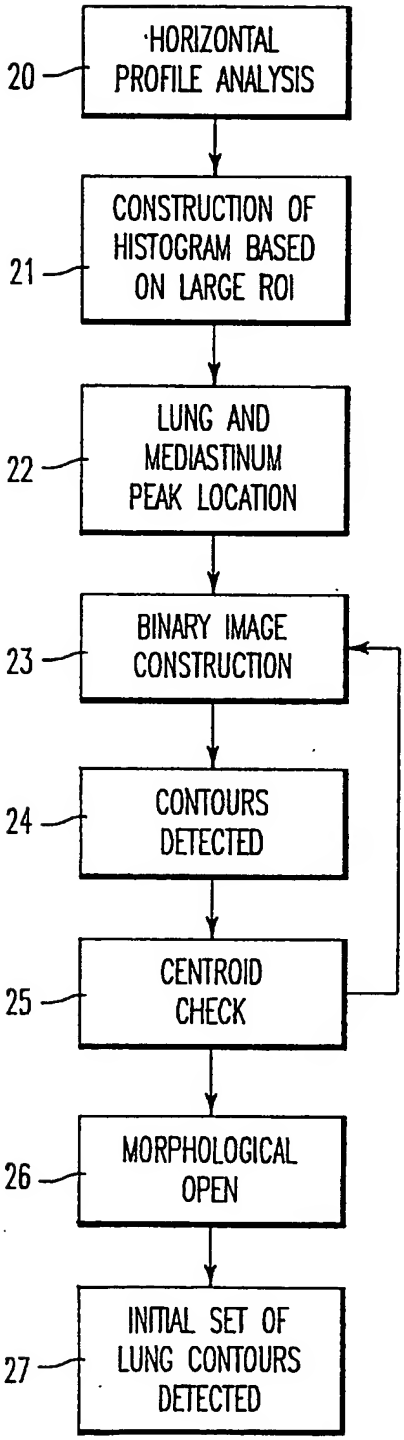
20
HORIZONTAL PROFILE ANALYSIS
21
CONSTRUCTION OF HISTOGRAM BASED ON LARGE ROI
22
LUNG AND MEDIASTINUM PEAK LOCATION
23
BINARY IMAGE CONSTRUCTION
24
CONTOURS DETECTED
25
CENTROID CHECK
26
MORPHOLOGICAL OPEN
27
INITIAL SET OF LUNG CONTOURS DETECTED

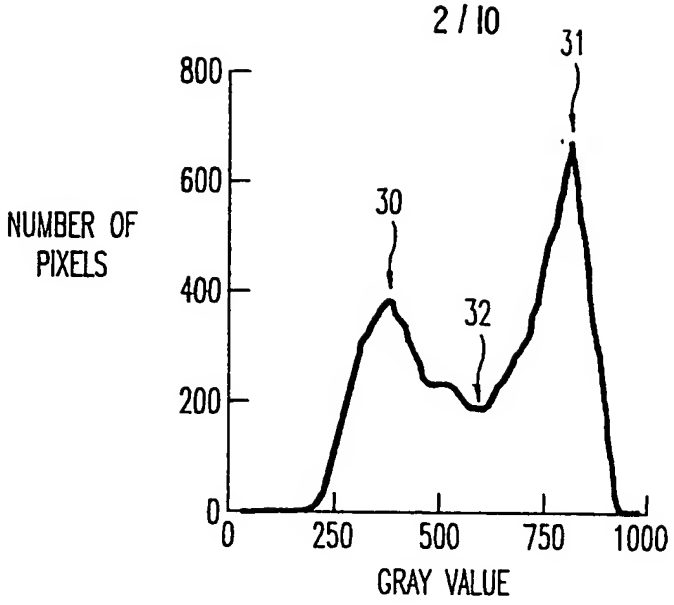
31
800
600
30
NUMBER OF PIXELS
400
32
200
0
0
250
500
750
1000
GRAY VALUE

FIG. 3

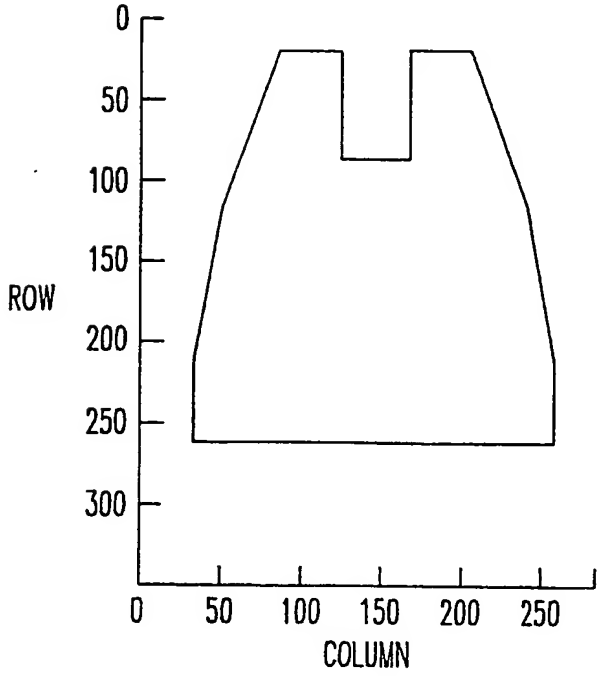
0
50
100
150
ROW
200
250
300
0
50
100
150
200
250
COLUMN

FIG. 5

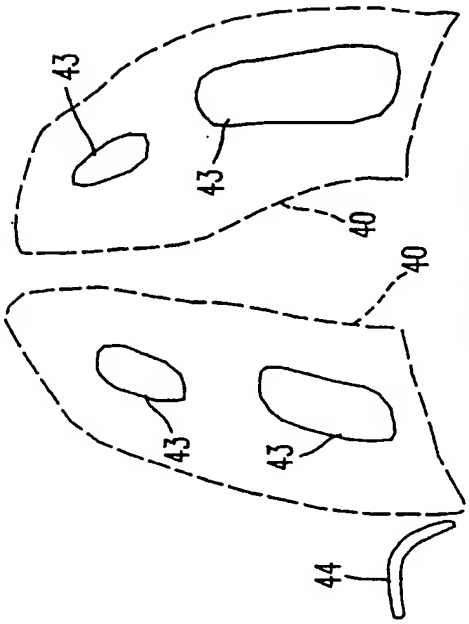

FIG. 4B

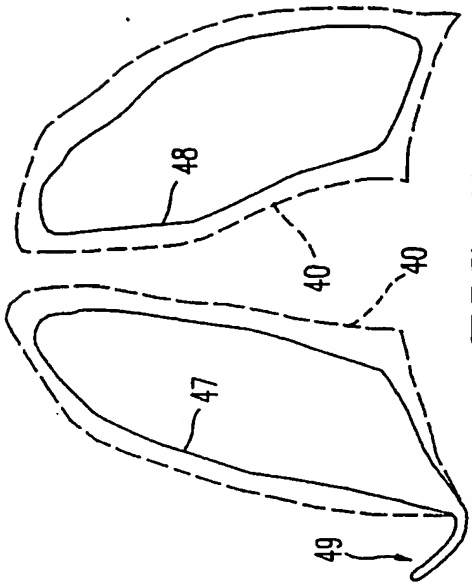

FIG. 4D

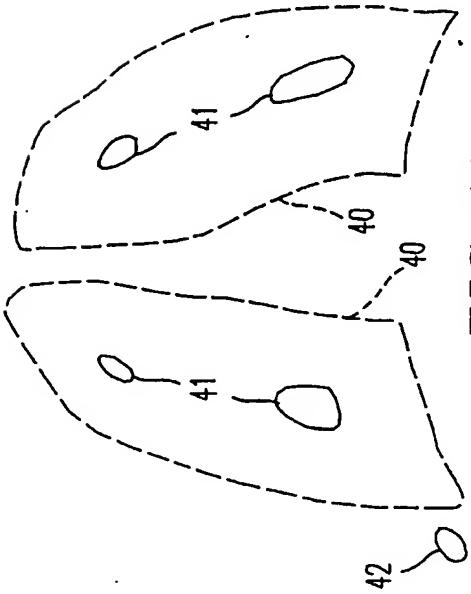

FIG. 4A

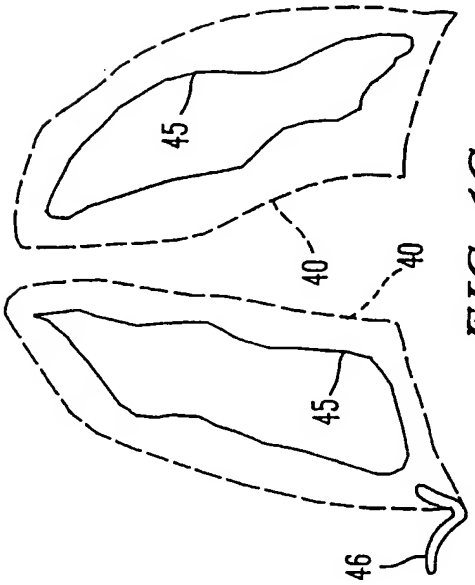

FIG. 4C

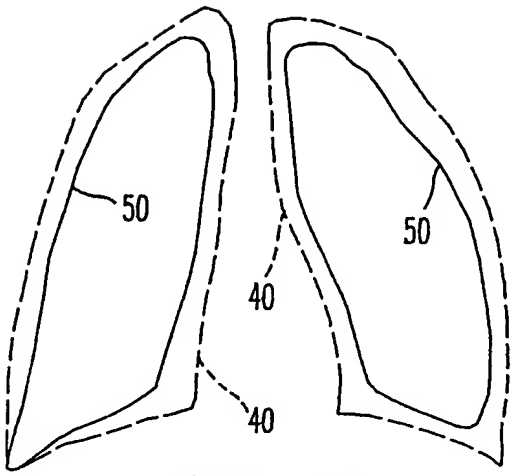

FIG. 4E

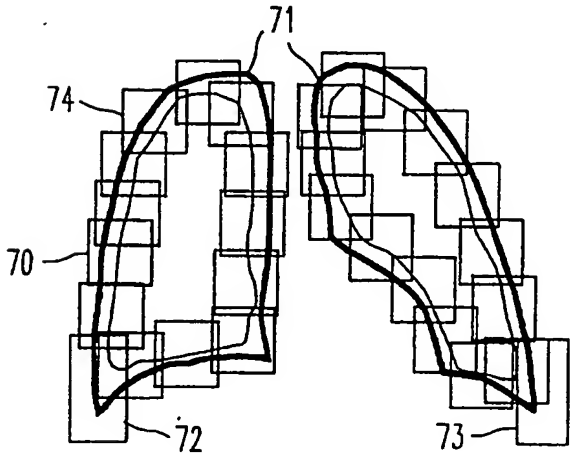

FIG. 7

FIG. 6

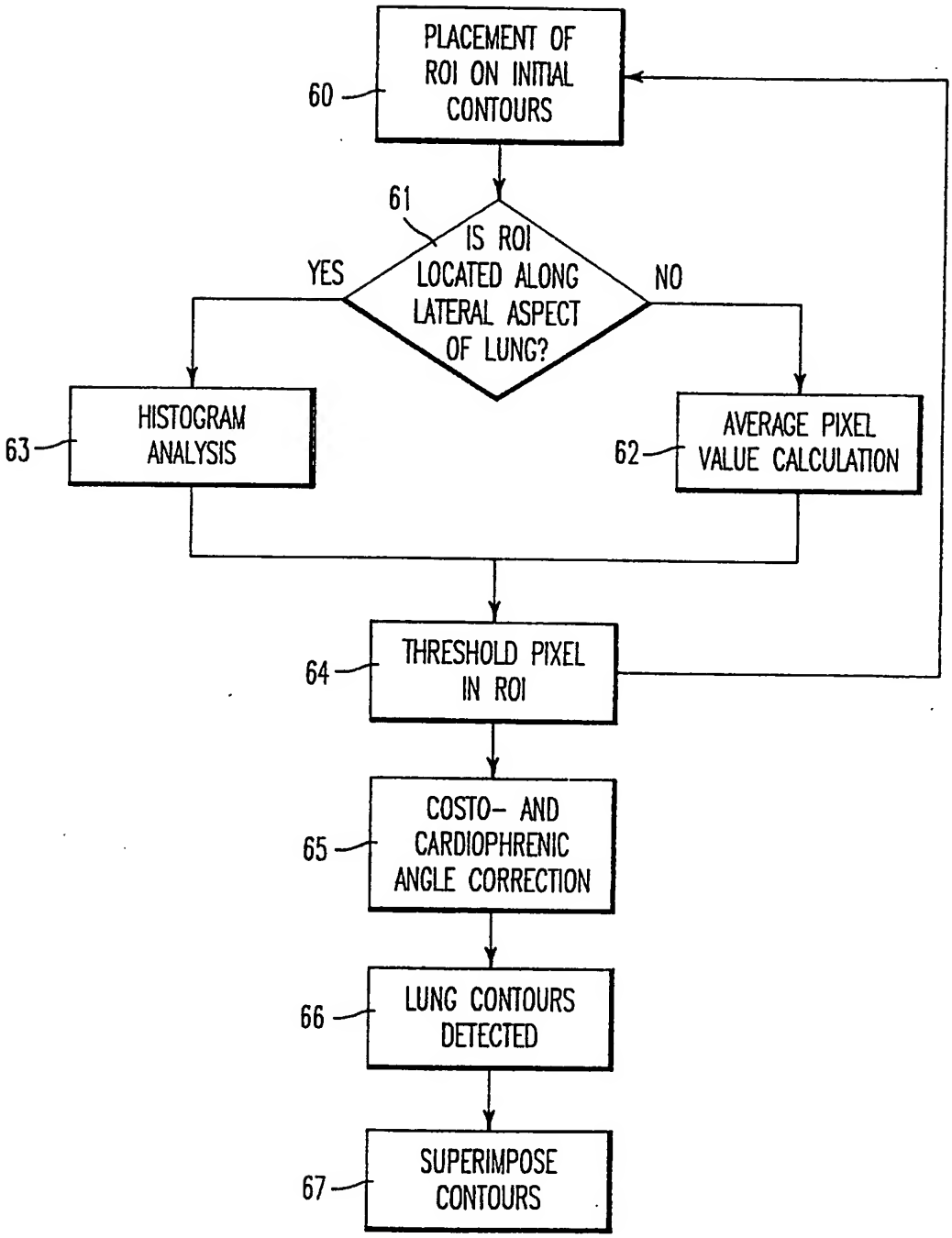
PLACEMENT OF ROI ON INITIAL CONTOURS
60
61
IS ROI LOCATED ALONG LATERAL ASPECT OF LUNG?
YES
NO
HISTOGRAM ANALYSIS
63
AVERAGE PIXEL VALUE CALCULATION
62
THRESHOLD PIXEL IN ROI
64
COSTO- AND CARDIOPHRENIC ANGLE CORRECTION
65
LUNG CONTOURS DETECTED
66
SUPERIMPOSE CONTOURS
67

FIG. 8A

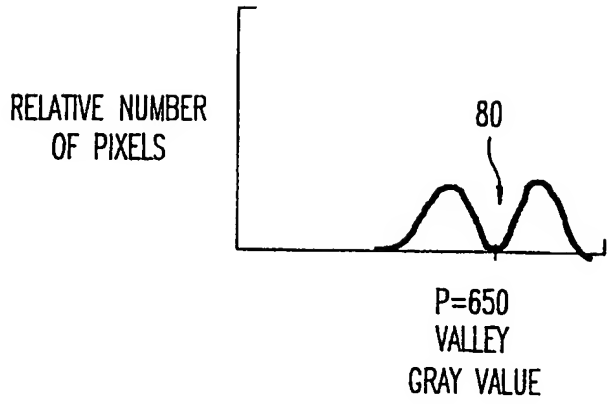
RELATIVE NUMBER
OF PIXELS
80
P=650
VALLEY
GRAY VALUE

FIG. 8B

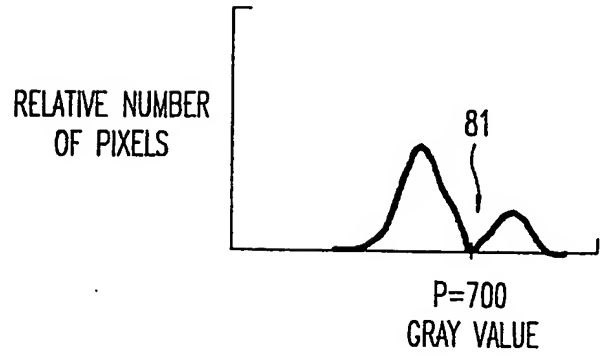
RELATIVE NUMBER
OF PIXELS
81
P=700
GRAY VALUE

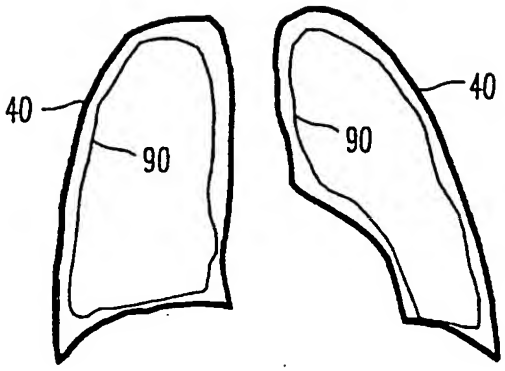

FIG. 9A

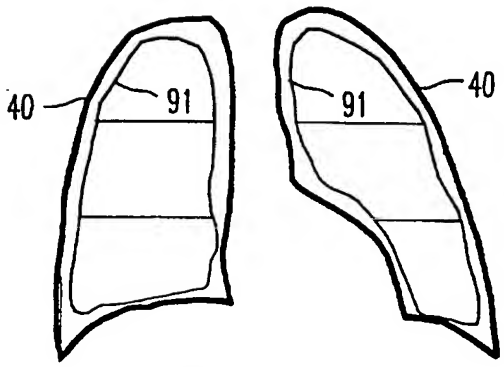

FIG. 9B

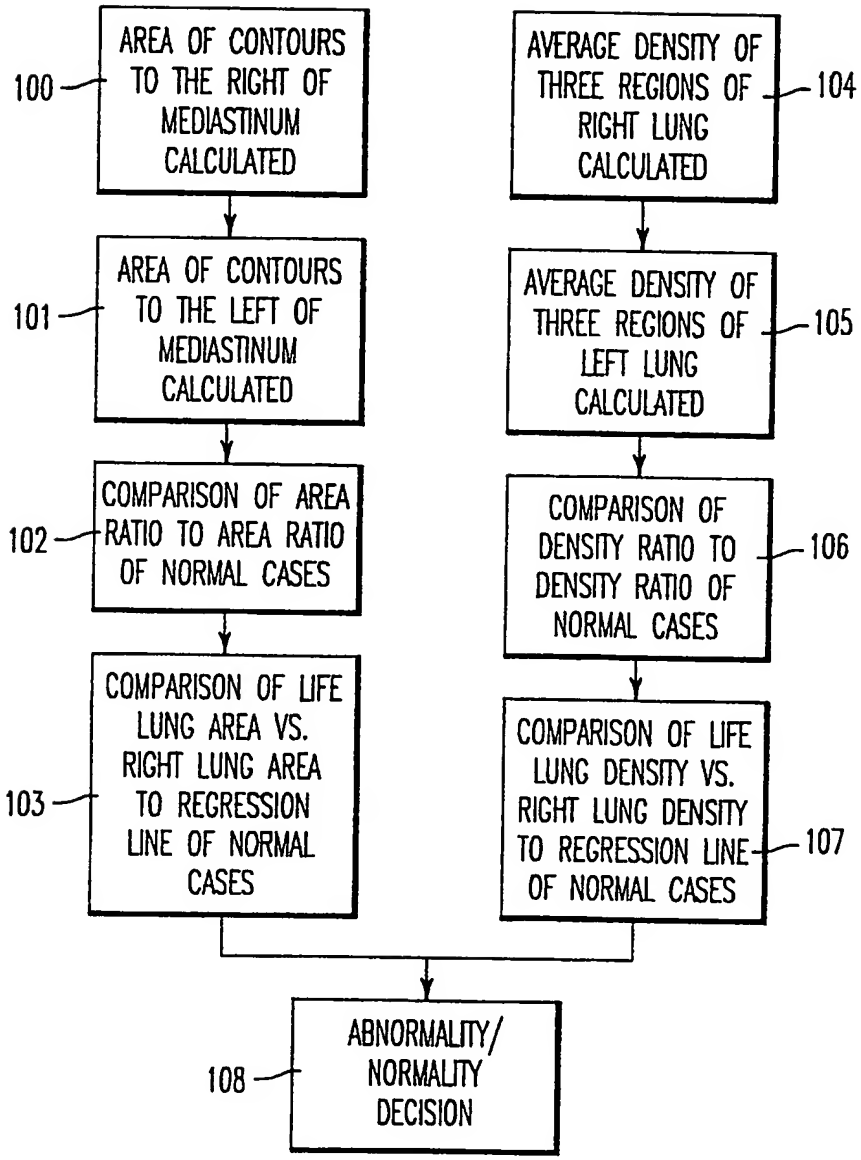
AREA OF CONTOURS TO THE RIGHT OF MEDIASTINUM CALCULATED
100
AREA OF CONTOURS TO THE LEFT OF MEDIASTINUM CALCULATED
101
COMPARISON OF AREA RATIO TO AREA RATIO OF NORMAL CASES
102
COMPARISON OF LIFE LUNG AREA VS. RIGHT LUNG AREA TO REGRESSION LINE OF NORMAL CASES
103
AVERAGE DENSITY OF THREE REGIONS OF RIGHT LUNG CALCULATED
104
AVERAGE DENSITY OF THREE REGIONS OF LEFT LUNG CALCULATED
105
COMPARISON OF DENSITY RATIO TO DENSITY RATIO OF NORMAL CASES
106
COMPARISON OF LIFE LUNG DENSITY VS. RIGHT LUNG DENSITY TO REGRESSION LINE OF NORMAL CASES
107
ABNORMALITY/ NORMALITY DECISION
108

FIG. 10

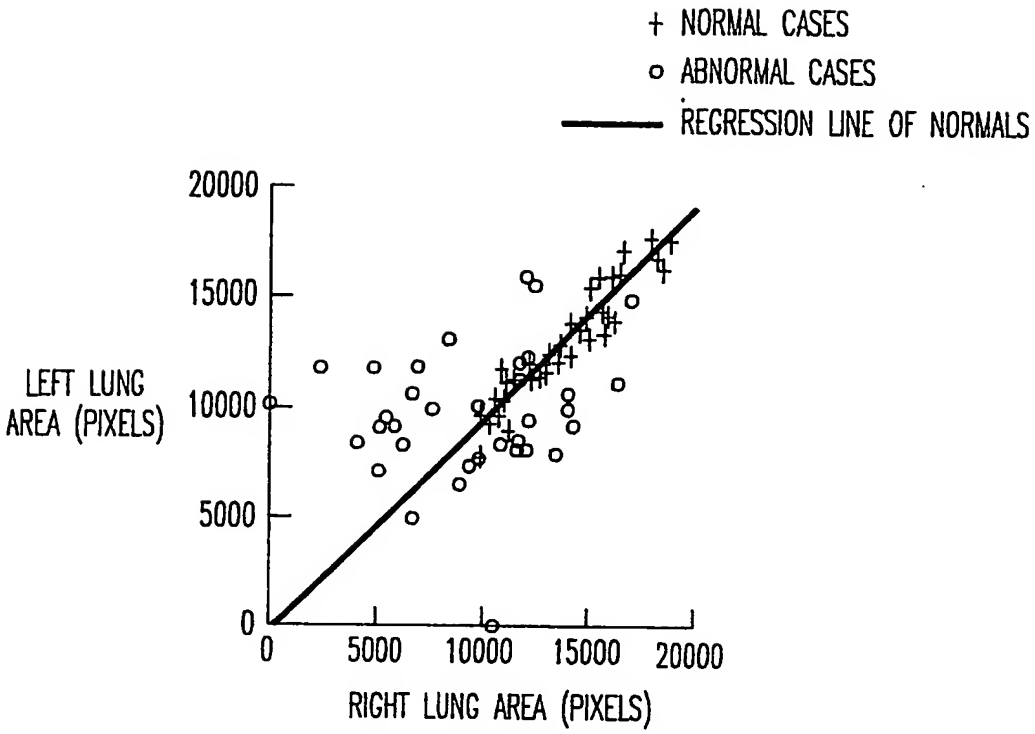
+ NORMAL CASES
o ABNORMAL CASES
REGRESSION LINE OF NORMALS
LEFT LUNG AREA (PIXELS)
20000
15000
10000
5000
0
0
5000
10000
15000
20000
RIGHT LUNG AREA (PIXELS)

FIG. 11

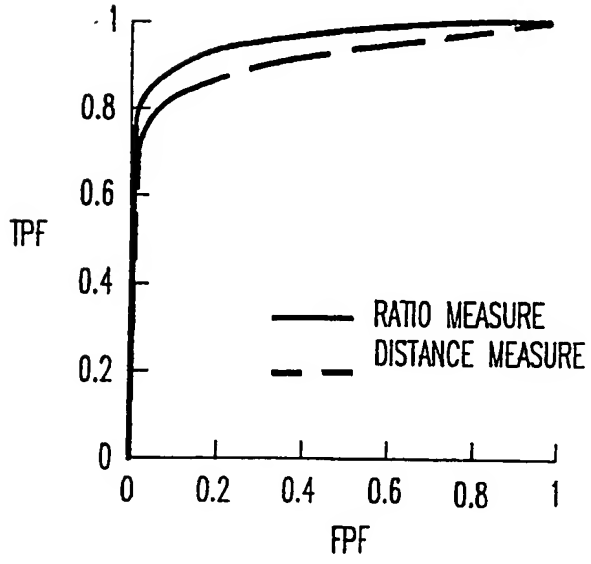
TPF
1
0.8
0.6
0.4
0.2
0
RATIO MEASURE
DISTANCE MEASURE
0
0.2
0.4
0.6
0.8
1
FPF

FIG. 12

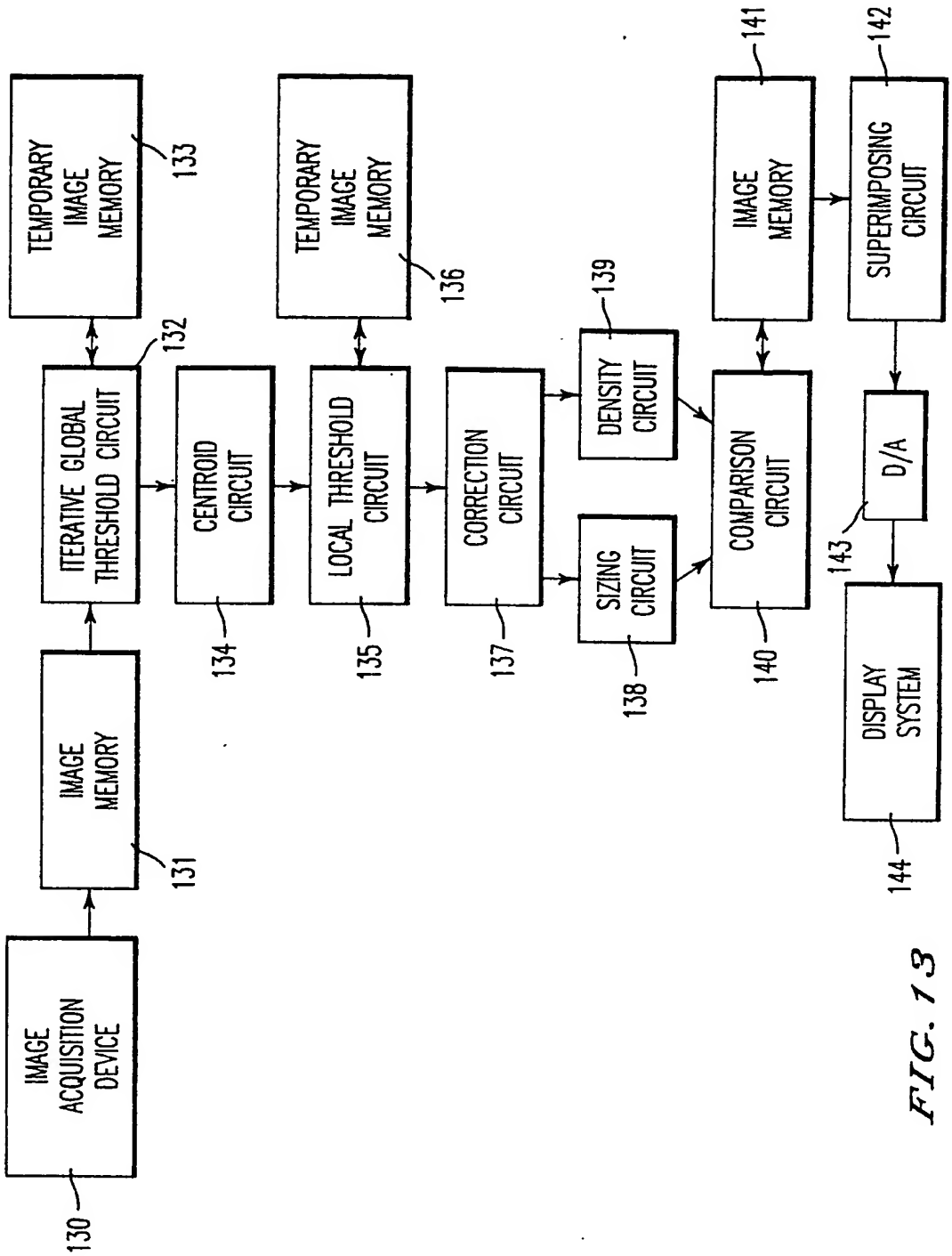
IMAGE ACQUISITION DEVICE
130
IMAGE MEMORY
131
ITERATIVE GLOBAL THRESHOLD CIRCUIT
132
TEMPORARY IMAGE MEMORY
133
CENTROID CIRCUIT
134
LOCAL THRESHOLD CIRCUIT
135
TEMPORARY IMAGE MEMORY
136
CORRECTION CIRCUIT
137
SIZING CIRCUIT
138
DENSITY CIRCUIT
139
COMPARISON CIRCUIT
140
IMAGE MEMORY
141
SUPERIMPOSING CIRCUIT
142
D/A
143
DISPLAY SYSTEM
144

FIG. 13

INTERNATIONAL SEARCH REPORT

International application No.
PCT/US94/13294

A. CLASSIFICATION OF SUBJECT MATTER

IPC(6) :G06K 9/00, 9/46, 9/48, 9/52, 9/38

US CL :382/6, 18, 19, 22, 28, 51

According to International Patent Classification (IPC) or to both national classification and IPC

B. FIELDS SEARCHED

Minimum documentation searched (classification system followed by classification symbols)

U.S. : 382/6, 18, 19, 22, 28, 51; 364/ 413.13, 413. 19, 413. 22, 413. 23

Documentation searched other than minimum documentation to the extent that such documents are included in the fields searched

Electronic data base consulted during the international search (name of data base and, where practicable, search terms used)

C. DOCUMENTS CONSIDERED TO BE RELEVANT

Category*	Citation of document, with indication, where appropriate, of the relevant passages	Relevant to claim No.
X, P ----- Y, P	US, A, 5,319,549 (KATSURAGAWA ET AL) 07 JUNE 1994, the abstract; Figs. 1, 2A-2C, 9A-9D; col. 2, line 13 - col. 3, line 10.	1-3, 18-21, 36-37 ----------4-17, 22-35, 38-43
X, P -----Y, P	US, A, 5,343,390 (DOI ET AL) 30 AUGUST 1994, the abstract, Figs. 1A-1B, 15A-15B, 16; col. 2, lines 1-57.	1-3, 18-21, 36-37 ---------- 4-17, 22-35, 38-43
X --- Y	US, A, 5,133,020 (GIGER ET AL) 21 JULY 1992, the abstract, Figs. 1-4, 6, 18, 19, 21a-21d; col. 2, line 32 - col. 3, line 21.	1-3 ----- 4-43

[X] Further documents are listed in the continuation of Box C. [ ] See patent family annex.

*	Special categories of cited documents:	"T"	later document published after the international filing date or priority date and not in conflict with the application but cited to understand the principle or theory underlying the invention
"A"	document defining the general state of the art which is not considered to be part of particular relevance	"X"	document of particular relevance; the claimed invention cannot be considered novel or cannot be considered to involve an inventive step when the document is taken alone
"E"	earlier document published on or after the international filing date	"Y"	document of particular relevance; the claimed invention cannot be considered to involve an inventive step when the document is combined with one or more other such documents, such combination being obvious to a person skilled in the art
"L"	document which may throw doubts on priority claim(s) or which is cited to establish the publication date of another citation or other special reason (as specified)	"&"	document member of the same patent family
"O"	document referring to an oral disclosure, use, exhibition or other means		
"P"	document published prior to the international filing date but later than the priority date claimed		

Date of the actual completion of the international search 04 APRIL 1995	Date of mailing of the international search report 11APR1995
Name and mailing address of the ISA/US Commissioner of Patents and Trademarks Box PCT Washington, D.C. 20231 Facsimile No. (703) 305-3230	Authorized officer PHUOC TRAN Telephone No. (703) 305-4900

Form PCT/ISA/210 (second sheet)(July 1992)*

INTERNATIONAL SEARCH REPORT

International application No.
PCT/US94/13294

C (Continuation). DOCUMENTS CONSIDERED TO BE RELEVANT

Category*	Citation of document, with indication, where appropriate, of the relevant passages	Relevant to claim No.
Y	US, A, 4,907,156 (DOI ET AL) 06 MARCH 1990, the abstract , Figs. 17, 18; col. 3, lines 1-37.	4-43
Y	Med. Phys. 17(3), May/June 1990, 1990 Am. Assoc. Med., "IMAGE FEATURE ANALYSIS AND COMPUTER-AIDED DIAGNOSIS IN DIGITAL RADIOGRAPHY: AUTOMATED ANALYSIS OF SIZES OF HEART AND LUNG IN CHEST IMAGES", Nakamori et al., pps. 342-350.	1-43
Y	Med. Phys. 15(4), July/August 1988, 1988 Am. Assoc. Phys. Med., "LOCALIZATION OF INTER-RIB SPACES FOR LUNG TEXTURE ANALYSIS AND COMPUTER-AIDED DIAGNOSIS IN DIGITAL CHEST IMAGES", Powell et al., pps. 581-587.	1-43

This Page is Inserted by IFW Indexing and Scanning Operations and is not part of the Official Record

BEST AVAILABLE IMAGES

Defective images within this document are accurate representations of the original documents submitted by the applicant.

Defects in the images include but are not limited to the items checked:

- ☑ BLACK BORDERS
- ☐ IMAGE CUT OFF AT TOP, BOTTOM OR SIDES
- ☑ FADED TEXT OR DRAWING
- ☑ BLURRED OR ILLEGIBLE TEXT OR DRAWING
- ☐ SKEWED/SLANTED IMAGES
- ☐ COLOR OR BLACK AND WHITE PHOTOGRAPHS
- ☐ GRAY SCALE DOCUMENTS
- ☐ LINES OR MARKS ON ORIGINAL DOCUMENT
- ☐ REFERENCE(S) OR EXHIBIT(S) SUBMITTED ARE POOR QUALITY
- ☐ OTHER: _____

IMAGES ARE BEST AVAILABLE COPY.
As rescanning these documents will not correct the image problems checked, please do not report these problems to the IFW Image Problem Mailbox.